INSTITUTE OF PHYSICS PUBLISHING JOURNAL OF PHYSICS: CONDENSED MATTER

J. Phys.: Condens. Matter **15** (2003) 5923–5932 PII: S0953-8984(03)64715-6

Formation and crystallization of CuZrHfTi bulk metallic glass under ambient and high pressures

Zhi Xin Wang[1], De Qian Zhao[1], Ming Xiang Pan[1], Wei Hua Wang[1,3], T Okada[2] and W Utsumi[2]

[1] Institute of Physics, Chinese Academy of Sciences, Beijing 100080, People's Republic of China
[2] Japan Atomic Energy Research Institute, SPring-8, Hyogo 679-5198, Japan

E-mail: whw@aphy.iphy.ac.cn

Received 11 June 2003, in final form 16 July 2003
Published 22 August 2003
Online at stacks.iop.org/JPhysCM/15/5923

Abstract

The formation of CuZrHfTi bulk metallic glasses (BMGs) and the crystallization of the typical $Cu_{60}Zr_{20}Hf_{10}Ti_{10}$ BMG under ambient conditions and high pressure have been investigated by differential scanning calorimetry, x-ray diffraction (XRD) and *in situ* synchrotron radiation XRD. The effects of high pressure on crystallization and formation of the CuZrHfTi alloy are discussed. The Kauzmann temperature, T_K, where the entropy of the undercooled liquid equals that of the crystal, is also determined to be 724 K. The T_K is compared with the experimentally observed rate-dependent glass transition, T_g. The kinetic study of the crystallization shows that the Cu-based BMG has much larger activation energies obtained using Kissinger analysis and is markedly different in crystallization kinetic behaviour compared to that of other BMGs with better glass forming abilities. An apparent correlation between crystallization temperature and activation energy is found in various metallic glasses. The correlation is discussed and connected with the thermal stability of metallic glasses.

(Some figures in this article are in colour only in the electronic version)

1. Introduction

Recently, various multicomponent metallic alloys were found to exhibit excellent glass forming ability (GFA) [1, 2]. Quantitative research activities on bulk metallic glasses (BMGs) reveal that they exhibit a wide supercooled liquid region, high thermal stability against crystallization and unique features [1]. Cu–Zr–Hf–Ti BMGs were developed in 2000 and they were found to have excellent mechanical properties, their fracture strength is above 2000 MPa [3]. Comparing with other BMG systems, such as Zr-based and Pd-based BMGs, the product cost of Cu-based

[3] Author to whom any correspondence should be addressed.

BMGs is much lower. In addition, they have high thermal stability against crystallization and the onset crystallization temperature, T_x, is about 750 K. Therefore, Cu-based BMGs have significant importance both in basic research and engineering aspects. However, the GFA of the Cu-based BMGs is not so good as that of Zr-based and Pd-based BMGs: the larger size of the BMGs limits us to 3–5 mm in diameter so far [3]. So the intriguing questions are: what are the main factors which govern the GFA and how to improve the GFA of the alloys. On the other hand, crystallization studies of metallic glasses are important for understanding the mechanisms of phase transformations far from equilibrium. The detailed investigation of the crystallization is also very important for evaluating the GFA of the melts, the thermal stability of the metallic glasses, and for producing controlled ultrafine microstructures from metallic glasses. The kinetic nature of crystallization provides a means of analysing the nucleation and dynamic change in the supercooled liquid state from the heating rate. High pressure can be applied to control the nucleation and growth in the undercooled melt, it can provide a useful way to study the crystallization mechanism of BMGs [4–6]. In fact, the crystallization of the BMG was found to be sensitive to the composition of the alloys and the external factors, for example, applied pressure and the heating rate [7–11]. However, the crystallization process of the BMGs is very complex and the effects of factors are numerous. The crystallization features of these BMGs are not understood very well. To better understand the GFA of metallic alloys, an important step is to develop a controlled method to examine the nucleation and growth of crystalline phases in the undercooled melt. The applied pressure can cause the melting point of most alloys to increase and leads to a larger undercooling of the liquid alloy. Therefore, applied pressure during the solidification process of a glass-forming alloy may provide a useful way to study the formation mechanism of the BMG.

In this paper, the formation and crystallization of CuZrHfTi BMG is studied at ambient and high pressure conditions using *in situ* synchrotron radiation x-ray diffraction (XRD). The kinetics of the crystallization behaviour of a typical $Cu_{60}Zr_{20}Hf_{10}Ti_{10}$ BMG is investigated by means of differential scanning calorimetry (DSC) and compared with other BMGs. The comparison shows that the Cu- and Fe-based BMGs have poor GFA compared to other BMGs but have very high thermal stability. An apparent correlation between crystallization temperature and activation energy is found in various BMGs. The correlation is discussed and connected with the thermal stability of metallic glasses.

2. Experimental details

CuZrHfTi BMG was prepared by melting a mixture of the element (with purity of about 99.99 at.%) in a Ti-gettered arc furnace and then cast in a water-cooled Cu mould to get a rod with a diameter of 3 mm. The phase evolution, melt and quench of the bulk glass forming alloy were studied by an *in situ* XRD method at SPring-8, the third-generation synchrotron facility in Japan. High-pressure and high-temperature conditions were generated using a cubic-type multianvil press (SMAP 180) installed on BL14B1 at SPring-8. The sample assembly was similar to that used in [12]. The sample capsule was made of pyrophyllite. A NiCr–NiAl thermocouple was brought into the pressurized zone near the sample and the absolute error in the temperature determination under applied pressure is about ± 2 K. NaCl powder was used as the pressure transmitting medium. The pressure was calibrated from the lattice constant of NaCl and the accuracy was better than ± 0.2 GPa. The sample was first subjected to high pressure and then heated to 1373 K and kept in these condition for 5 min. After this, the heating electrical current was switched off and the sample was naturally cooled under HP. Because the sample was covered with thick pyrophyllite and ZrO_2 with low thermal conductivity, the solidifying heat release condition for the molten sample was very poor compared with that of

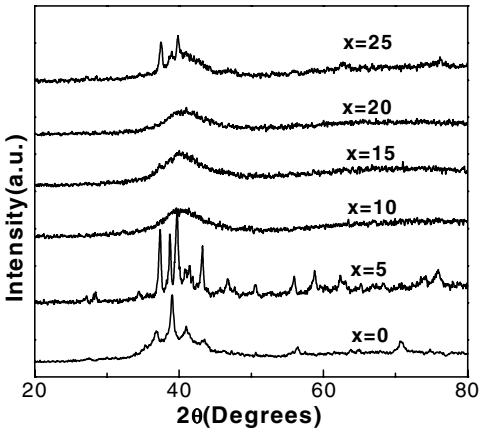

Figure 1. X-ray diffraction patterns of $Cu_{60}Zr_{30-x}Hf_xTi_{10}$ BMGs.

the sample die-cast in a water-cooled Cu mould. An energy dispersive method was utilized using white x-rays with an energy of 30–150 keV. The diffracted x-ray was detected by a solid state Ge detector and the diffraction angle 2θ was fixed to 3°. The structure of the sample was also checked by XRD using a Rigaku Rapid-XRD diffractometer with Cu Kα radiation. The DSC measurements were carried out under a purified argon atmosphere in a Perkin-Elmer DSC7 at a heating rate ϕ ranging from 5 to 80 K min^{-1}. The calorimeter was calibrated for temperature and energy at various heating rates with high purity indium and zinc. The values of the glass transition temperature T_g, and the onset temperature for the crystallization peak T_x, were determined from the DSC traces with an accuracy of ± 1 K.

3. Results and discussion

Figure 1 shows the XRD patterns of cylindrical $Cu_{60}Zr_{30-x}Hf_xTi_{10}$ rods, which were cast under ambient pressure at the same cooling rate of about 100 K s^{-1}. It was found that the GFA of the alloy depends on the content of Hf. For small Hf addition (0–5 at.% Hf, shown in figure 1), the alloy is not fully amorphous. It is worth noting that the as-cast 3 mm rod of $Cu_{60}Zr_{30}Ti_{10}$ ($x = 0$) exhibits obvious crystalline phases in figure 1, but an amorphous structure was shown in [3]. The difference is due to the formation of BMGs depending on the cooling rate, the purity of the elements and the quality of the vacuum in the casting furnace. Therefore, for the same alloy with the same preparation method, the results could be different because the cooling rate, the purity of elements and the vacuum quality of the casting furnace could be different. We used elements with relatively low purity and low vacuum in our preparation method. When the content of Hf reaches 10–20 at.%, no distinct crystalline peaks can be seen in the XRD curves, indicating that a fully glass phase is obtained without obvious crystalline phases in the sample, with diameter up to 3 mm. However, when the content of Hf is more than 25 at.%, some crystalline peaks appear again in the XRD pattern. Too little or too much Hf addition leads to precipitation of crystalline phases, and a fully metallic glass cannot be obtained for the alloy under the same processing conditions. Therefore, an appropriate Hf addition can improve the GFA of the Cu–Zr–Ti alloy. The results are consistent with our previous work which shows that the correct addition of elements can markedly improve the GFA and properties of the various BMGs [13–15]. The liquid temperature T_l determined by differential thermal analysis is 1189 K. The reduced glass transition temperature T_{rg} ($T_{rg} = T_g/T_l$) is 0.63. According

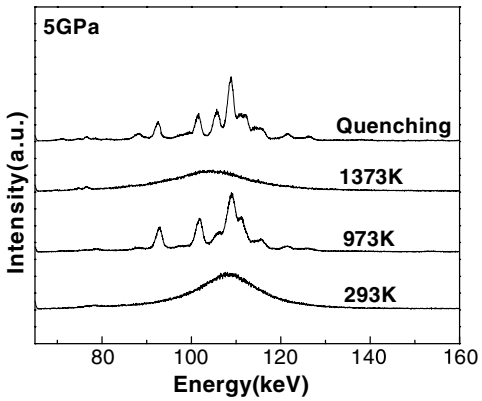

Figure 2. Synchrotron XRD patterns of the $Cu_{60}Zr_{20}Hf_{10}Ti_{10}$ BMG heated at various temperatures and quenching rates under 5 GPa.

to Turnbull's criterion [16], a liquid with $T_g/T_l \geqslant 2/3$ can only crystallize within a very narrow temperature range, and thus can be easily undercooled at a low cooling rate into the glassy state. The value of T_g/T_l is close to $2/3$, indicating the $Cu_{60}Zr_{20}Hf_{10}Ti_{10}$ alloy has a good GFA. The Hf addition experiment seems to further confirm the validity of the 'confusion principle' [18]. However, it would be interesting to note that the enthalpy of mixing between Cu and Zr (-23 kJ mol^{-1}) [17] is smaller than that of Cu–Hf (-17 kJ mol^{-1}) [17], indicating that the addition of Hf should increase the whole enthalpy of mixing of the alloy, that is, reduce the amorphization driving force. On the other hand, Hf and Zr have the same atomic radii, which means that Hf addition is not expected to cause an increase of melt viscosity in the supercooled liquid through an increase in the different atomic sizes of the components. The effective role of Hf in enhancement of the GFA of the Cu-based BMG does not satisfy the empirical roles for BMG formation [1]. More work is needed to clarify this phenomenon.

Figure 2 shows the synchrotron XRD patterns of the $Cu_{60}Zr_{20}Hf_{10}Ti_{10}$ BMG *in situ* measured under 5 GPa at various temperatures. The crystallization of the $Cu_{60}Zr_{20}Hf_{10}Ti_{10}$ BMG prepared at ambient conditions (with a cooling rate of about 100 K s^{-1}) was studied by an *in situ* XRD method at SPring-8 under high pressure. The BMG is fully crystallized at 973 K during the increasing temperature process. Up to 1373 K, the alloy is totally melted. The melt is quenched to room temperature under 5 GPa (the quenching rate is about 20 K s^{-1}). The existence of evident peaks in the XRD pattern of the quenched sample indicates that a fully amorphous phase cannot be obtained during the high pressure quench. The alloy quenched at different pressures is presented in figure 3. The sample under ambient pressure was prepared by casting in a water-cooled Cu mould (the cooling rate is about 100 K s^{-1}). Fully amorphous alloys cannot be obtained by quenching at the same cooling rate at 5 and 8 GPa. Pressure in this range does not obviously improve the GFA of the alloy, while in a Zr–Ti–Cu–Ni–Be glass forming alloy, pressure in the range of 1–10 GPa can significantly enhance the GFA [19], as shown in figure 3(b). With the same cooling rate, a fully amorphous alloy can be obtained under 7.6 GPa, while it cannot be obtained under 4.5 GPa for the $Zr_{46.75}Ti_{8.25}Cu_{7.5}Ni_{10}Be_{27.5}$ (vit4) alloy. The result indicates the effect of pressure on GFA depends on the applied pressure range. Because the GFA of $Cu_{60}Zr_{20}Hf_{10}Ti_{10}$ is much smaller than that of vit4, a much higher pressure may be needed to favour the glass formation of the Cu-based alloys.

We chose $Cu_{60}Zr_{20}Hf_{10}Ti_{10}$ which has the best GFA of the alloy systems to study the crystallization and effects of high pressure on the GFA of Cu-based BMGs. Figure 4 presents

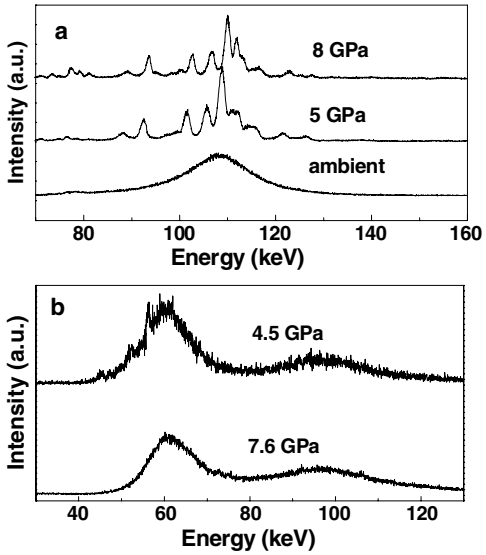

Figure 3. (a) Synchrotron XRD patterns of the $Cu_{60}Zr_{20}Hf_{10}Ti_{10}$ BMG quenching under various pressures. (b) Synchrotron XRD patterns of the vit4 BMG quenching under pressures of 4.5 and 7.6 GPa.

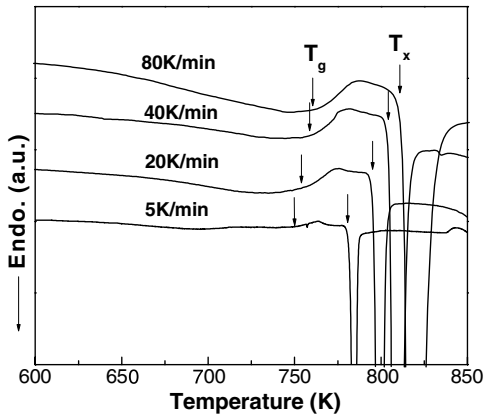

Figure 4. DSC curves for the $Cu_{60}Zr_{20}Hf_{10}Ti_{10}$ BMG at different heating rates.

DSC traces of the BMG at various heating rates of 5, 20, 40 and 80 K min^{-1}. The endothermic characteristic of a glass transition followed by an exothermic crystallization peak at a higher temperature can be found in all DSC curves. The onset glass transition temperature T_g, the onset crystallization temperature T_x, the crystallization peak temperature T_{p1} and supercooled liquid region ($\Delta T = T_x - T_g$) for BMG at the heating rate of 20 K min^{-1} are 754, 797, 800 and 43 K, respectively. The obtained parameters of T_g, T_x, T_{p1} and ΔT at different heating rates are listed in table 1. All the T_g, T_x, T_{p1} and ΔT are increased with increasing heating rate. The shift to higher temperature of T_g and T_x, shows that the glass transition and the crystallization behave in a markedly kinetic nature. The dependence of T_g and T_x on the heating rate, shown in figure 5, follows Lasock's relationship [20], $T = A + B \ln \phi$, where A and B are constants. The value of A and B are different for the glass transition and crystallization reaction. The

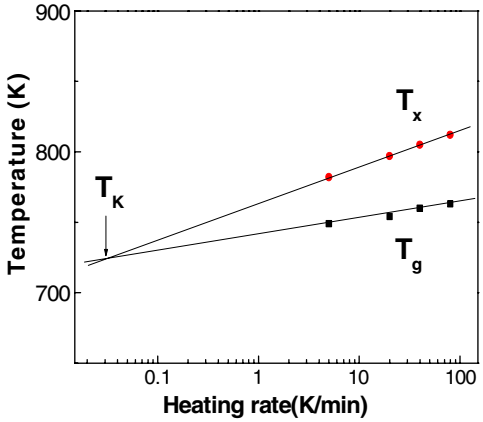

Figure 5. The glass transition temperature and the onset temperature of crystallization obtained from the DSC measurements for the $Cu_{60}Zr_{20}Hf_{10}Ti_{10}$ BMG as a function of the heating rate.

Table 1. Thermodynamic and kinetic parameters of the $Cu_{60}Zr_{20}Hf_{10}Ti_{10}$ BMG.

Heating rate (ϕ)	T_g (K)	T_x (K)	T_{p1} (K)	ΔT (K)
5	749	782	785	33
20	754	797	800	43
40	760	805	808	45
80	763	812	818	49

values of A and B are 743.6 and 4.24 for T_g, and 771.7 and 8.99 for T_x, respectively. It can be deduced that the crystallization shows a stronger dependence on heating rate than that of the glass transition. When extrapolating the dependence of T_g and T_x on heating rate, the two curves intersect at a temperature of 724 K (shown in figure 5), which, within experiment error, is equal to the ideal glass transition temperature (Kauzmann temperature), T_K [21]. The extrapolated heating rate required to reach T_K is 0.03 K min^{-1}. The difference between T_g (at 20 K min^{-1}) and T_K is 30 K, which is much smaller than that for ZrTiCuNiBe BMG (65 K) [11].

The activation energy E_{p1} for the crystallization reaction is determined by Kissinger's equation [22]:

$$\ln \frac{T^2}{\phi} = \frac{E}{k_B T} + C, \tag{1}$$

where k_B is Boltzmann's constant. The Kissinger plot of the crystallization temperatures for the BMG is shown in figure 6. The E_{p1} is determined to be 4.51 eV. Table 2 shows the values of E_{p1} and the thermodynamic and kinetic parameters for various BMGs. Compared to Zr-, Pd- and Pr-based BMGs, which have excellent GFA, the $Cu_{60}Zr_{20}Hf_{10}Ti_{10}$ BMG similar to Fe-, Co-based metallic glasses has a much larger value of activation energy E_{p1}, high thermal stability and poor GFA. It indicates that those alloys with excellent GFA do not necessarily imply a high thermal stability. This phenomenon has also been found in the same alloy system, such as the vitalloy system [27]. For example, the $Zr_{41}Ti_{14}Cu_{12.5}Ni_{10}Be_{22.5}$ BMG (vit1) represents one of the best glass formers, but its thermal stability is substantially reduced compared to vit4. Conversely, vit4 exhibits the best thermal stability in the alloy system, yet its GFA is greatly reduced [27]. Figure 7 presents the relation between T_{p1} and E_{p1}. It is seen

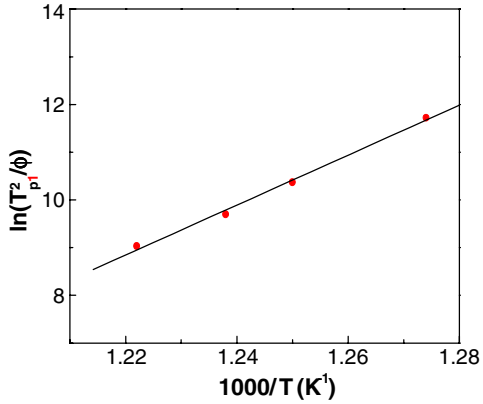

Figure 6. Kissinger's plots of the peak temperature obtained from the DSC measurements for the $Cu_{60}Zr_{20}Hf_{10}Ti_{10}$ BMG.

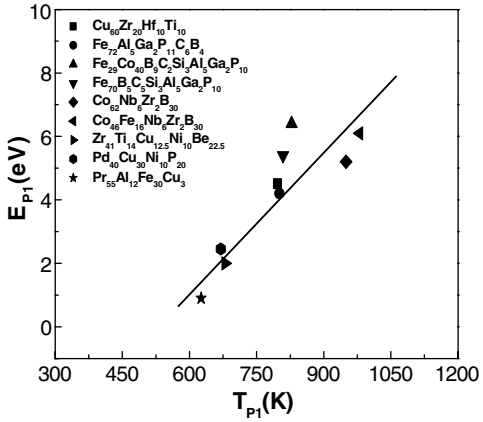

Figure 7. The comparison of the values of T_{p1} and E_{p1} for various metallic glasses. The full line is used to guide the eye.

that E_{p1} roughly increases with the increase in T_{p1}. In the process of crystallization, the atoms participating in the crystallization will acquire additional energy to form critical nuclei. This energy is captured through collisions. The activation energy, E_{p1}, can be interpreted as the additional energy that an atom must acquire in order to be a part of the critical nuclei [22, 28]. The correlation between onset crystallization temperature and E_{p1} can be understood from the barrier energy for crystallization. The metallic glasses with high crystallization temperatures mean that the atoms need larger additional energy to become a part of the critical nuclei, which need a larger critical size to become a nucleation site. This leads to a high energy being needed for activating the nucleation and growth process during the crystallization.

Figure 8 shows the synchrotron XRD patterns of a $Cu_{60}Zr_{20}Hf_{10}Ti_{10}$ BMG at various temperatures under 8.0 GPa. Up to 893 K, the amorphous structure is retained without clear indications of crystallization. At 913 K, there are some very small and broadened crystalline peaks appearing. With the increase in temperature, the crystalline peaks become narrower in width and higher in intensity, up to 1173 K, when crystallization of the BMG is finished. The crystallization temperature is different at 5 GPa (it is about 893 K). Some small

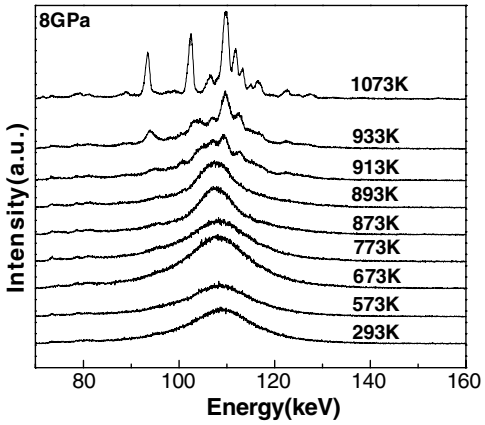

Figure 8. Synchrotron XRD patterns of the $Cu_{60}Zr_{20}Hf_{10}Ti_{10}$ BMG heated at various temperatures and quenching under 8 GPa.

Table 2. A comparison of the values of E_g, E_{p1}, T_{rg} (represented the glass forming ability of an alloy [16]) and other thermodynamic and kinetic parameters obtained for various BMGs.

BMG	T_g (K)	T_x (K)	ΔT (K)	T_m (K)	T_{rg}	E_{p1} (eV)	References
$Cu_{60}Zr_{20}Hf_{10}Ti_{10}$[a]	754	797	43	1133	0.63	4.51	This work
$Fe_{72}Al_5Ga_2P_{11}C_6B_4$[a]	736	801	65	—	—	4.2	[8]
$Fe_{29}Co_{40}B_9C_2Si_3Al_5Ga_2P_{10}$[b]	782	828	46	1320	0.57	6.4	[23]
$Fe_{70}B_5C_5Si_3Al_5Ga_2P_{10}$[b]	755	809	54	1280	0.59	5.4	[23]
$Co_{62}Nb_6Zr_2B_{30}$[c]	900	950		1436	0.63	5.2	[23]
$Co_{46}Fe_{16}Nb_6Zr_2B_{30}$[c]	892	980	88	1420	0.63	6.1	[23]
$Zr_{41}Ti_{14}Cu_{12.5}Ni_{10}Be_{22.5}$[a]	623	680	57	937	0.63	2.0	[7]
$Pd_{40}Cu_{30}Ni_{10}P_{20}$[a]	575	670	95	804	0.67	2.45	[24, 25]
$Pr_{55}Al_{12}Fe_{30}Cu_3$[c]	551	626	75	850	0.64	0.90	[26]

[a] Heating rate is 40 K min^{-1}.
[b] Heating rate is 20 K min^{-1}.
[c] Heating rate is 10 K min^{-1}.

crystalline peaks appear at 893 K. The crystallization temperature of the sample under 8 GPa is higher than under 5 GPa, indicating that pressure impedes the crystallization detected by XRD. The crystallization of BMGs involving nucleation and growth is a diffusion-controlled process. A lot of experimental work shows that the crystallization of the multicomponent BMGs in the low temperature region of the supercooled liquid region is by a growth-control mechanism which needs a long-range atomic diffusion due to a large composition difference between the amorphous phase and its products [27, 29–31]. High pressure promotes a short-range atomic rearrangement in metallic glass by the reduction of the free volume because of compression [21, 22]. However, the high pressure makes the long-range atomic diffusion more difficult in the BMGs and the growth of the nucleus is inhibited by the extremely slow mobility [29, 32]. This leads to the increase of crystallization temperature detected by XRD. Figure 9 shows the product crystalline phases of the $Cu_{60}Zr_{20}Hf_{10}Ti_{10}$ BMG under different pressures. It can be found that the main phase peaks for 5 GPa correspond well to the phase peaks for 8 GPa. The glass alloy crystallizes into a mainly $Cu_{10}Zr_7$-type crystalline phase.

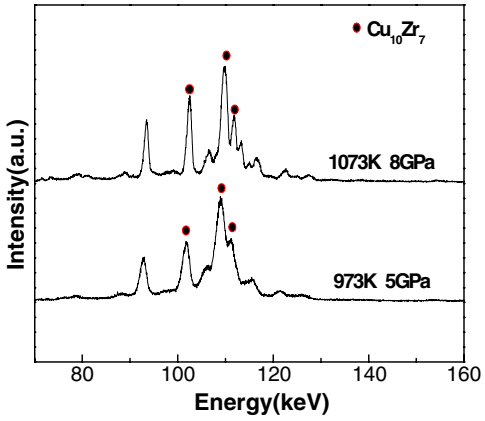

Figure 9. Synchrotron XRD patterns of crystallization of the $Cu_{60}Zr_{20}Hf_{10}Ti_{10}$ BMG under various pressures.

4. Conclusions

The formation of CuZrHfTi BMGs under ambient conditions and high pressure is studied. An accurate Hf addition can improve the GFA of the Cu–Zr–Ti alloy and pressure does not obviously improve the GFA of the alloy. However, high pressure can increase the crystallization temperature of the BMG, and the BMG crystallizes into a $Cu_{10}Zr_7$-type crystalline phase under high pressure. From the kinetic study, the glass transition and the crystallization are found to have a markedly kinetic nature: the Kauzmann temperature, T_K, is then determined to be 724 K. The activation energy of the crystallization of the glass is 4.51 eV, much larger than that of other BMGs. This is attributed to the high thermal stability of the Cu-based BMG. The crystallization activation energy is found to have a correlation with crystallization temperature in various metallic glasses.

Acknowledgments

The authors are grateful for the financial support of the National Natural Science Foundation of China (grant no 59925101 and 50031010), Chinesisch-Deutsches Zentrum Für Wissenschaftsfoerderung (grant no GZ032/7) and the Key Project of the Beijing Science and Technology Program (contract no H02040030320). WHW thanks the Japanese Sciences Promotion Society (JSPS) for financial support.

References

[1] Inoue A 1995 *Mater. Trans. JIM* **36** 866
[2] Johnson W L 1999 *MRS Bull.* **24** 42
[3] Inoue A, Zhang W, Zhang T and Kurosaka K 2001 *Mater. Trans. JIM* **42** 1805
[4] Wang W K, Iwasaki H and Fukamichi K 1980 *J. Mater. Sci.* **15** 2701
[5] Shen Z Y, Chen G Y, Zhang Y and Yin X J 1989 *Phys. Rev.* B **39** 2714
[6] Yousuf M and Rajan K G 1984 *J. Mater. Sci. Lett.* **3** 149
[7] Zhuang Y X, Wang W H and Zhao D Q 1999 *Appl. Phys. Lett.* **75** 2392
[8] Mitrovic N, Roth S and Eckert J 2001 *Appl. Phys. Lett.* **78** 2145
[9] Wang W H, Zhuang Y X, Pan M X and Yao Y S 2000 *J. Appl. Phys.* **88** 3914
[10] Pan M X, Wang J G, Yao Y S and Wang W H 2001 *J. Phys.: Condens. Matter* **13** 589

[11] Busch R, Kim Y J and Johnson W L 1995 *J. Appl. Phys.* **77** 4039
[12] Utsumi W, Funakoshi K, Urakawa S, Yamakata M, Tsuji K, Konishi H and Shimomura O 1998 *Rev. High Pressure Sci. Technol.* **7** 1484
[13] Wang W H, Bian Z, Wen P, Zhang Y, Pan M X and Zhao D Q 2002 *Intermetallic* **10** 1249
[14] Wang W H, Wei Q and Bai H Y 1997 *Appl. Phys. Lett.* **71** 58
Zhang Y, Zhao D Q, Wang R J, Pan M X and Wang W H 2000 *Mater. Trans. JIM* **41** 1427
[15] Hu Y, Zhao Y H, Pan M X, Zhao D Q and Wang W H 2003 *Mater. Lett.* **57** 2698
[16] Turnbull D 1969 *Contemp. Phys.* **10** 437
[17] De Boer F R, Boom R, Mattens W C M, Miedema A R and Niessen A K 1988 *Cohesion in Metals* (Amsterdam: North-Holland)
[18] Greer A L 1993 *Nature* **366** 303
Greer A L 1995 *Science* **267** 1947
[19] Wang W H, Wang R J, Zhao D Q and Yao Y S 2001 *Appl. Phys. Lett.* **79** 1106
Wang W H, Zhao D Q and Utsumi W 2003 at press
[20] Lasocka T M 1976 *Mater. Sci. Eng.* **23** 173
[21] Okamoto P R, Lam N Q and Rehn L E 1999 *Solid State Physics* vol 52, ed H Ehrenrein and F Spapen (San Diego, CA: Academic) pp 1–135
[22] Kissinger H E 1956 *J. Res. Natl Bur. Stand.* **57** 217
[23] Borrego J M, Conde A, Roth S and Eckert J 2002 *J. Appl. Phys.* **92** 2073
Borrego J M, Conde C F, Conde A, Roth S, Grahl H, Ostwald A and Eckert J 2002 *J. Appl. Phys.* **92** 6607
[24] Nishiyama N and Inoue A 1999 *Acta Mater.* **47** 1487
[25] Inoue A 1998 *Bulk Amorphous Alloys, Practical Characteristics and Applications, Materials Science Foundation* (Switzerland: Trans Tech) p 6
[26] Li Z, Bai H Y, Pan M X, Zhao D Q and Wang W H 2003 *Acta Phys. Sin.* **52** 652
[27] Waniuk T, Schroers J and Johnson W L 2003 *Phys. Rev.* B **67** 184203
[28] Ligero R A, Vázquez J, Villares P and Jiménez-garay R 1989 *Mater. Lett.* **8** 6
[29] Wang W H, Wei Q and Fridrich S 1998 *Phys. Rev.* B **57** 8211
[30] Schroers J, Wu Y, Busch R and Johnson W L 2001 *Acta Mater.* **49** 2773
[31] Schroers J, Masuhr A and Johnson W L 1999 *Phys. Rev.* B **60** 11855
[32] Ruitenberg G, De Hey P, Sommer F and Sietsma J 1997 *Phys. Rev. Lett.* **79** 4830